

Attitude Synchronization and Stabilization for Multi-Satellite Formation Flying with Advanced Angular Velocity Observers

Belkacem Kada¹, Khalid Munawar², Muhammad Shafique Shaikh³

Aerospace Engineering Department, King Abdulaziz University, Jeddah, KSA¹

Electrical & Computer Engineering Department, King Abdulaziz University, Jeddah, KSA^{2,3}

Abstract—This paper focuses on two aspects of satellite formation flying (SFF) control: finite-time attitude synchronization and stabilization under undirected time-varying communication topology and synchronization without angular velocity measurements. First, a distributed nonlinear control law ensures rapid convergence and robust disturbance attenuation. To prove stability, a Lyapunov function involving an integrator term is utilized. Specifically, attitude synchronization and stabilization conditions are derived using graph theory, local finite-time convergence for homogeneous systems, and LaSalle's non-smooth invariance principle. Second, the requirements for angular velocity measurements are loosened using a distributed high-order sliding mode estimator. Despite the failure of inter-satellite communication links, the homogeneous sliding mode observer precisely estimates the relative angular velocity and provides smooth control to prevent the actuators of the satellites from chattering. Simulations numerically demonstrate the efficacy of the proposed design scheme.

Keywords—Attitude synchronization; coordinated control; finite-time control; high-order sliding mode observer; inter-satellite communication links; leader-following consensus; switching communication topology

I. INTRODUCTION

Distributed satellite systems (DSS) are an enabling technology for future distributed space missions since they are designed to interact as multi-agent systems for consensus tracking or formation keeping. DSS are deployed at different altitudes and in various configurations (e.g., formations, clusters, swarms, or cancellations) to accomplish distributed space missions like constellation [1], Earth observation [2], remote sensing [3], communication services [4], and meteorology and environmental tasks [5].

Satellite formation flying (SFF) is an attractive concept of DSS flying in prescribed orbits at a fixed separation distance for a given period. This concept enables flexible, reliable, and low-cost space missions [6,7]. However, SFF control requires tight interactions between participating satellites. Relative motion determination is essential for formation keeping and on-orbit reconfiguration. Therefore, SFF systems must meet strict attitude synchronization and tracking requirements before deployment.

The leader-follower-based attitude synchronization has received growing attention in recent years. Several synchronization protocols for SFF systems under fixed and

switching communication topologies have been reported in the literature. Zhou et al. [8] proposed a finite-time control law that guaranteed the coordination of a spacecraft formation under a fixed communication graph. The control law integrated a sliding-mode-based observer, allowing individual satellites to estimate the desired angular velocity. Although the control scheme showed a fast convergence rate, the control torques exhibited chattering effects, which can harm the actuators. Zhao and Jia [9] used a non-singular terminal sliding mode to design a distributed adaptive attitude synchronization algorithm. The chattering of the controllers was avoided using a boundary layer approach. The control algorithm was validated using only a fixed communication graph, which can restrain its ability when switching communication topologies. The attitude synchronization problem for a distributed SFF was investigated by Wang et al. [10]. The authors designed a free-reference attitude control algorithm under communication constraints, demonstrating an asymptotic convergence with an extensive settling time. Zhang et al. [11] discussed the application of integral sliding mode control to the problem of adaptive attitude tracking. The control input was smoothed via the boundary layer method but at the cost of settling time response. Zhang et al. [12] proposed a finite-time attitude synchronization and orbit-tracking control scheme that demonstrated robustness against node failures and torque disturbances. However, the simulations showed a slow convergence rate and high oscillation torques. Combining LQR and robust control approaches, Liu et al. [13] alleviated the effect of nonlinearities and parametric uncertainties on the performance of SFF attitude alignment. The control scheme was validated for a fixed communication topology presenting an asymptotic convergence. Liu et al. [14] designed an adaptive coordinated attitude synchronization control algorithm and a distributed observer for spacecraft formation over a switching network. Although simulations verified the performance of the proposed control scheme, the observer provided an asymptotic convergence to the leader reference attitude, which can degrade formation performance. Lu and Liu [15] further investigated attitude synchronization under switching topologies. The authors proposed a control scheme to guarantee attitude tracking under global and local failures of inter-satellite communication links (ISCLs). However, the consensus protocols showed an asymptotic convergence and required angular speed measurements.

Similarly, Zhang et al. [16] proposed a finite-time distributed attitude synchronization algorithm that requires the availability of the relative angular velocity for all the following satellites, which often leads to a heavy burden of ISCLs and time-consuming control. Zhang et al. [17] used the set theory to develop a new attitude of cooperative control for different SFF structures. Under fixed-time communication topology, the control design worked adequately for the leader-following and leaderless formation structures; however, neither dynamic communication graphs nor external disturbances were considered. Finally, Wei et al. [18] presented a comprehensive overview of the state-of-the-art communication satellite systems in their survey paper. The authors showed that recent publications have focused on designing synchronization techniques for SFF systems with node failures. They concluded that high-accuracy synchronization could be achieved using two-way ISCLs (i.e., undirected communication graphs) and precise observation techniques.

This paper provides solutions to two open problems above finite-time attitude synchronization under ISCLs breaks and robust relative angular velocity estimation. The first problem is solved by designing a distributed attitude synchronization algorithm using a Lyapunov function that involves an integrator term enabling a fast convergence rate. In contrast to the finite-time synchronization schemes available in the literature, the proposed algorithm allows attitude synchronization with time-varying communication graphs. As for the second problem, a high-order sliding mode differentiator estimates the relative angular velocity, guarantees formation robustness, and avoids chattering effects. The distributed observer helps relax the communication topology requirements and reduce the ISCLs burden. Most of the existing velocity-free or observer-based protocols have a slow convergence rate, lack of robustness, or perform only for fixed-time communication topology (e.g., [8,19-23]).

The outline of this paper is given as follows. Section II presents the preliminaries of this work and describes quaternion-based satellite attitude dynamics. A distributed finite-time attitude synchronization controller and relative angular velocity estimator are designed in Section III. Numerical simulations are carried out in Section IV to demonstrate the effectiveness and robustness of the proposed control scheme. Finally, Section V concludes the work.

II. PRELIMINARIES AND DYNAMIC MODELING

A. Graph Theory and Preliminaries

The leader-follower consensus approach is considered in this study to design distributed attitude synchronization and stabilization (ASS) protocols. The satellites are regarded as followers denoted by $'i = 1, 2, \dots, n'$, and the leader (i.e., desired attitude) is represented by $'i = 0'$. The ISCLs topology is modeled by a graph $\mathcal{G} = (\mathcal{V}, \mathcal{E}, \mathcal{A})$ where $\mathcal{V} = (v_1, v_2, \dots, v_n)$ denotes the vertices set, $\mathcal{E} \subseteq \mathcal{V} \times \mathcal{V}$ represents the edge set, and $\mathcal{A} = (a_{ij} \geq 0) \in \mathbb{R}^{n \times n}$ is the adjacent matrix corresponding to the graph \mathcal{G} . If a follower-satellite $'i'$ is connected to the leader, then the connection weight is represented by $a_{i0} > 0$; otherwise $a_{i0} = 0$. The

Laplacian matrix $\mathcal{L} = (\ell_{ij}) \in \mathbb{R}^{n \times n}$ associated to the graph \mathcal{G} is defined as

$$\mathcal{L} = \mathcal{D} - \mathcal{A}, \mathcal{D} = \text{diag}(d_{ii}), d_{ii} = \sum_{j \in N_j} a_{ij} \quad (1)$$

where $N_j = \{j | j \in \mathcal{V}, (j, i) \in \mathcal{E}\}$ represents the neighborhood set of a node $'i'$

Lemma 1 [24]: If the matrix \mathcal{L} is associated with a connected undirected graph \mathcal{G} , then its spectrum is given as

- $\lambda_1(\mathcal{L}) = 0$ is a simple eigenvalue of \mathcal{L} with a corresponding eigenvector $\mathbf{1}_n = [1, \dots, 1]_n^T$.
- All nonzero eigenvalues $\lambda_i(\mathcal{L})$ for $1 < i \leq n$ have positive real parts.
- $0 \leq \lambda_2(\mathcal{L}) \leq \dots \leq \lambda_n(\mathcal{L})$.

Lemma 2 [24]: According to the extension theorem, the following condition holds for any integral function f

$$\left\| \int_a^b f(t) dt \right\|_2 \leq (b - a) \|f(t)\|_\infty \quad (2)$$

Definition 1: Let $\mathbf{x} \in \mathbb{R}^n$ be a fixed, measurable function with l_1 -norm $\|\mathbf{x}\|_1 = \max|\mathbf{x}|$ and define an integral operator $L_K \mathbf{x}(t) = \int_X \mathbf{K} \mathbf{x}(t) dt$. Then

$$\|L_K\|_{HS} = \|\mathbf{K}\|_2^2 \quad (3)$$

where X is a compact with kernel \mathbf{K} and HS denotes Hilbert Schmidt norm.

B. Satellite Attitude Kinematics and Dynamics

Let $\bar{\mathbf{q}}_i = [q_{0i} \ \mathbf{q}_i]^T \in \mathbb{R}^4$ and $\boldsymbol{\omega}_i \in \mathbb{R}^3$ denote an i^{th} satellite's orientation and angular velocity within an SFF orbiting in an inertial frame. The nonlinear attitude kinematics and dynamics models are given by

$$\dot{\bar{\mathbf{q}}}_i = -\frac{1}{2} \boldsymbol{\Omega}(\boldsymbol{\omega}) \bar{\mathbf{q}}_i \quad (4)$$

$$\mathbf{J}_i \dot{\boldsymbol{\omega}}_i = -\boldsymbol{\omega}_i \times \mathbf{J}_i \boldsymbol{\omega}_i + \boldsymbol{\tau}_i + \mathbf{d}_i$$

with $\boldsymbol{\Omega}(\boldsymbol{\omega}) \in \mathbb{R}^{4 \times 4}$ is defined as

$$\boldsymbol{\Omega}(\boldsymbol{\omega}) = \begin{bmatrix} 0 & \omega_3 & -\omega_2 & \omega_1 \\ -\omega_3 & 0 & \omega_1 & \omega_2 \\ \omega_2 & -\omega_1 & 0 & \omega_3 \\ -\omega_1 & -\omega_2 & -\omega_3 & 0 \end{bmatrix}$$

\mathbf{J}_i , $\boldsymbol{\tau}_i$, \mathbf{d}_i denote the inertia tensor, torque vector, and external disturbances vector, respectively. Using the matrix $\mathbf{Q}_i(\mathbf{q}_i) = \mathbf{q}_{0i} \mathbf{I}_{3 \times 3} - \mathbf{q}_i^\times$ the model (4) can be rewritten as follows

$$\begin{aligned} \dot{\mathbf{q}}_i &= -\mathbf{Q}(\mathbf{q}_i) \boldsymbol{\omega}_i \\ \dot{q}_{0i} &= -\frac{1}{2} \boldsymbol{\omega}_i^T \mathbf{q}_i \end{aligned} \quad (5)$$

$$\mathbf{J}_i \dot{\boldsymbol{\omega}}_i = -\boldsymbol{\omega}_i^\times \mathbf{J}_i \boldsymbol{\omega}_i + \boldsymbol{\tau}_i + \mathbf{d}_i$$

where \mathbf{q}_i^\times is the skew-symmetric cross-product matrix and $\mathbf{I}_{3 \times 3}$ denotes a three-dimensional identity matrix. The satellites' angular velocities and external disturbances in the model (5) are bounded, as shown in assumptions 1 and 2 [11].

Assumption 1: $\|\omega_i\|_2 \leq \rho$ and $\|\dot{\omega}_i\|_2 \leq \delta$ with $\rho, \delta \in \mathbb{R}^+$.

Assumption 2: There exist $\gamma_0, \gamma_1 \in \mathbb{R}^+$ such that $\|d_i\|_2 \leq \gamma_1 \|\omega_i\|_2 + \gamma_0$

The control objective here is to design consensus protocols (control torques τ_i) such that the attitude synchronization of SFF orbiting with time-varying interaction topologies is achieved in a finite time. Thus, $\forall x_i^0 \in D \subset \mathbb{R}^3$ there exists a synchronization time t_s for which

$$\begin{cases} \lim_{t \rightarrow t_s} \|\mathbf{q}_i - \mathbf{q}_d\|_2 = 0 \\ \lim_{t \rightarrow t_s} \|\omega_i - \omega_d\|_2 = 0 \end{cases} \quad (6)$$

where \mathbf{q}_d and ω_d denote the desired orientations and angular velocities.

III. SYNCHRONIZATION CONTROL LAW DESIGN

A. SFF Attitude Synchronization under Undirected Time-Varying Interaction Topology

Consider the case of a SFF where at least one follower satellite is connected to the virtual leader. The following finite-time distributed torque law is considered for attitude synchronization of the i^{th} satellite I the SFF

$$\begin{aligned} \tau_i = & \omega_i^{\times} J_i \omega_i - J_i Q_i \omega_i - \\ & k J_i \{ [\sum_{j \in \mathcal{N}} a_{ij} (\mathbf{q}_i - \mathbf{q}_j) + a_{i0} (\mathbf{q}_i - \mathbf{q}_d)] + \\ & [\sum_{j \in \mathcal{N}} a_{ij} (\omega_i - \omega_j) + a_{i0} (\omega_i - \omega_d)] \} \end{aligned} \quad (7)$$

with $k \in \mathbb{R}^+$ is a control parameter.

Theorem 1: Consider a satellite formation flying under an undirected time-varying communication graph and suppose that the dynamics described in Eq. (5) are undisturbed and satisfy assumption 1. The control law (7) guarantees the finite-time convergence of the formation satellites' states to the desired attitude and achieves the formation consensus (6) if there exists a positive-definite symmetric matrix \mathbf{M} and a control gain k satisfying the following conditions.

$$\begin{cases} \mathbf{M} = \mathbf{L} + \text{diag}(a_{i0}) \\ k > \frac{1}{\lambda_{\min}(\mathbf{M})} \end{cases} \quad (8)$$

Proof - Define the absolute quaternion and angular velocity tracking errors as follows

$$\begin{cases} \mathbf{q}_{ei} = \mathbf{q}_d^{\times} \mathbf{q}_i \\ \omega_{ei} = \omega_i - \omega_d \end{cases} \quad (9)$$

Let $\mathbf{q}_e = [\mathbf{q}_{e1}^T, \dots, \mathbf{q}_{en}^T]^T$, $\omega_e = [\omega_{e1}^T, \dots, \omega_{en}^T]^T$, $\mathbf{J} = \text{diag}\{\mathbf{J}_1, \dots, \mathbf{J}_n\}$, and $\mathbf{Q}_e = \text{diag}\{\mathbf{Q}_1, \dots, \mathbf{Q}_n\}$. Using the control law (7), the extension, to n satellites, of the undisturbed form of the torque equation in the model (5) gives

$$J \dot{\omega}_e = -J Q_e \omega_e - k J (\mathbf{M} \otimes \mathbf{I}_3) (\mathbf{q}_e + \omega_e) \quad (10)$$

where \otimes denotes the Kronecker product and \mathbf{I}_3 denotes the (3x3) identity matrix.

To reach the consensus (6) in finite time, consider the following candidate Lyapunov function with an integrator term

$$V = \frac{1}{2} \left[(\omega_e + \mathbf{q}_e) + \int_0^t (\omega_e + \mathbf{q}_e) d\tau \right]^T (\mathbf{M} \otimes \mathbf{I}_N) \left[(\omega_e + \mathbf{q}_e) + \int_0^t (\omega_e + \mathbf{q}_e) d\tau \right] \quad (11)$$

For simplicity, we define a matrix $\bar{\mathbf{M}} = (\mathbf{M} \otimes \mathbf{I}_N)$. Using Eq. (10), the time derivative of the function (11), along with system (5), can be written as

$$\begin{aligned} \dot{V} = & [-k \bar{\mathbf{M}} (\omega_e + \mathbf{q}_e) + (\omega_e + \mathbf{q}_e)]^T \bar{\mathbf{M}} \\ & \left[(\omega_e + \mathbf{q}_e) + \int_0^t (\omega_e + \mathbf{q}_e) d\tau \right] \\ = & -k (\omega_e + \mathbf{q}_e)^T \bar{\mathbf{M}}^T \bar{\mathbf{M}} (\omega_e + \mathbf{q}_e) \\ & + (\omega_e + \mathbf{q}_e)^T \bar{\mathbf{M}} (\omega_e + \mathbf{q}_e) \\ & - k (\omega_e + \mathbf{q}_e)^T \bar{\mathbf{M}}^T \bar{\mathbf{M}} \int_0^t (\omega_e + \mathbf{q}_e) d\tau + \\ & + (\omega_e + \mathbf{q}_e)^T \bar{\mathbf{M}} \int_0^t (\omega_e + \mathbf{q}_e) d\tau \end{aligned} \quad (12)$$

Since \mathbf{M} is symmetric, then $\bar{\mathbf{M}}^T \bar{\mathbf{M}} = \bar{\mathbf{M}}^2$. With $\lambda_{\min}(\bar{\mathbf{M}}^2) = \lambda_{\min}^2(\bar{\mathbf{M}}) = \lambda_{\min}^2(\mathbf{M})$ and $\lambda_{\max}(\bar{\mathbf{M}}^2) = \lambda_{\max}^2(\mathbf{M}) = \lambda_{\max}^2(\mathbf{M})$, expression (12) can be bounded as follows

$$\begin{aligned} \dot{V} \leq & - (k \lambda_{\min}(\mathbf{M}^2) - \lambda_{\min}(\mathbf{M})) \|\omega_e + \mathbf{q}_e\|_2^2 \\ & - (k \lambda_{\max}(\mathbf{M}^2) - \lambda_{\max}(\mathbf{M})) \|(\omega_e + \mathbf{q}_e)^T\|_1 \|(\omega_e + \mathbf{q}_e)^T\|_{\infty} \\ \leq & - \lambda_{\min}(\mathbf{M}) (k \lambda_{\min}(\mathbf{M}) - 1) \|\omega_e + \mathbf{q}_e\|_2^2 \\ & - \lambda_{\max}(\mathbf{M}) (k \lambda_{\max}(\mathbf{M}) - 1) \|(\omega_e + \mathbf{q}_e)\|_1 \|(\omega_e + \mathbf{q}_e)\|_{\infty} \end{aligned} \quad (13)$$

Thus if $k > 1/\lambda_{\min}(\mathbf{M})$, then

$$\dot{V} \leq -\lambda_{\min}(\mathbf{M}) (k \lambda_{\min}(\mathbf{M}) - 1) \|\omega_e + \mathbf{q}_e\|_2^2 \quad (14)$$

It follows that $\dot{V} \leq 0$. To prove that V will decrease to zero in finite time, \dot{V} will also satisfy

$$\dot{V} \leq -\lambda_{\max}(\mathbf{M}) (k \lambda_{\max}(\mathbf{M}) - 1) \|(\omega_e + \mathbf{q}_e)\|_1 \|(\omega_e + \mathbf{q}_e)\|_{\infty} \quad (15)$$

According to lemma 2, with the use of equation (11), the function V satisfies

$$\begin{aligned} V \leq & \frac{\lambda_{\max}(\mathbf{M})}{2} \left\| (\omega_e + \mathbf{q}_e) + \int_0^{t_s} (\omega_e + \mathbf{q}_e) d\tau \right\|_2^2 \\ \leq & \frac{\lambda_{\max}(\mathbf{M})}{2} \left(\|(\omega_e + \mathbf{q}_e)\|_2^2 + \left\| \int_0^{t_s} (\omega_e + \mathbf{q}_e) d\tau \right\|_2^2 \right) \\ \leq & \frac{\lambda_{\max}(\mathbf{M})}{2} \left(\|(\omega_e + \mathbf{q}_e)\|_1^2 + t_s^2 \|(\omega_e + \mathbf{q}_e)\|_{\infty}^2 \right) \\ \leq & \frac{t_s^2 \lambda_{\max}(\mathbf{M})}{2} \|(\omega_e + \mathbf{q}_e)\|_1^2 \|(\omega_e + \mathbf{q}_e)\|_{\infty}^2 \end{aligned} \quad (16)$$

where t_s denotes the settling time. It results from Eq. (15) and (16) that

$$\dot{V} \leq -\lambda_{\max}(\mathbf{M}) \left(\frac{\lambda_{\max}(\mathbf{M})}{\lambda_{\min}(\mathbf{M})} - 1 \right) \frac{\sqrt{2}\sqrt{V}}{\sqrt{t_s \lambda_{\max}(\mathbf{M})}} = -\alpha \sqrt{V} \quad (17)$$

which implies that for $\alpha = \frac{\sqrt{2}}{\sqrt{t_s}} \sqrt{\lambda_{\max}(\mathbf{M})} \left(\frac{\lambda_{\max}(\mathbf{M})}{\lambda_{\min}(\mathbf{M})} - 1 \right) > 0$, $V(t) \rightarrow 0$ as $t \rightarrow t_s$.

Finally, the settling time t_s is computed from the integration of Eq. (17) as follows

$$\sqrt{V(t)} \leq \sqrt{V(0)} - \frac{\alpha t_s}{2} \quad (18)$$

Using equation (11) at $t = 0$, the settling time t_s is given as

$$t_s = \frac{\sqrt{2(\boldsymbol{\omega}_e(0)+\mathbf{q}_e(0))^T(\mathbf{M}\otimes\mathbf{I}_N)(\boldsymbol{\omega}_e(0)+\mathbf{q}_e(0))}}{\sqrt{\lambda_{\max}(\mathbf{M})\left(\frac{\lambda_{\max}(\mathbf{M})}{\lambda_{\min}(\mathbf{M})}-1\right)}} \quad (19)$$

Thus, $\mathbf{q}_i \rightarrow \mathbf{q}_d$ and $\boldsymbol{\omega}_i \rightarrow \boldsymbol{\omega}_d$ in finite time for $t \geq t_s$.

End of proof.

B. Attitude Synchronization with High-Order Sliding Mode Estimator

In this subsection, a distributed angular velocity observer is introduced to reduce the number of ISCLs and guarantee the robustness of the SFF against loss of communication. First, a finite-time high-order sliding mode differentiator is designed to provide follower satellites with an accurate estimate of the desired angular velocity $\hat{\boldsymbol{\omega}}_i$. To do so, we define the following non-empty sliding mode function.

$$\mathbf{s}(t) = (\mathbf{s}_1^T, \mathbf{s}_2^T, \dots, \mathbf{s}_n^T)^T \quad (20)$$

where $\mathbf{s}_i \in \mathbb{R}^3$ denotes a sliding mode manifold for satellite 'i'. The sliding surface \mathbf{s}_i is defined by an integral sliding mode function as

$$\mathbf{s}_i = \mathbf{e}_{\omega,i} + \int_0^t \mathbf{e}_{\omega,i}(\tau) d\tau \quad (21)$$

with

$$\mathbf{e}_{\omega,i} = \sum_{j \in \mathcal{N}} [a_{ij}(\boldsymbol{\omega}_i - \boldsymbol{\omega}_j) + a_{i0}(\boldsymbol{\omega}_i - \boldsymbol{\omega}_d)] \quad (22)$$

Lemma 1 [25]: Consider a continuous function $f(t)$ with the time-derivative $f^{(r)}(t)$ has a Lipschitz constant $L > 0$ (i.e., $f^{(r)}(t) \leq L$), where r is the relative degree of $\mathbf{s}(t)$. The following high-order sliding mode differentiator produces accurate estimations of $f(t)$ and its successive time derivatives $f^{(k)}(t)$ ($k = 1, \dots, r - 1$) in finite time

$$\begin{cases} \dot{z}_0 = z_1 + \mu_0 |z_0 - f(t)|^{\frac{r-1}{r}} \\ \dot{z}_1 = z_2 + \mu_1 |z_0 - f(t)|^{\frac{r-2}{r-1}} \\ \vdots \\ \dot{z}_{r-2} = z_{r-1} + \mu_{r-2} |z_0 - f(t)|^{\frac{1}{2}} \\ \dot{z}_{r-1} = z_r + \mu_{r-1} \text{sign}(z_0 - f(t)) \end{cases} \quad (23)$$

where z_i ($i = 0, \dots, r$) denote the differentiator states and μ_i define the differentiator parameters. With $z_r = 0$, the differentiator (23) guarantees that $z_0 \rightarrow \hat{f}_i$ and $z_k \rightarrow \hat{f}_i^{(k)}$ ($k = 1, \dots, r - 1$) converge in finite time.

With $f(t) = s_{i,j}(t)$ where 'i' = 1, ..., n' denotes satellite 'i' and 'j' = 1, ..., 3' denotes motion direction, $\hat{\boldsymbol{\omega}}_{i,j} = z_0$ and $\hat{\boldsymbol{\omega}}_{i,j}^{(k)} = z_i^{(k)}$ ($k = 1, \dots, r - 1$) converge in finite time. We note that $\hat{\boldsymbol{\omega}}_{i,j}^{(k)}$ are the successive time-derivatives of the estimate $\hat{\boldsymbol{\omega}}_{i,j}^{(k)}$.

Second, under the results above, the control law (7) is redesigned as follows

$$\begin{aligned} \boldsymbol{\tau}_i = & \boldsymbol{\omega}_i^\times \mathbf{J}_i \boldsymbol{\omega}_i - \mathbf{J}_i \mathbf{Q}_i [\hat{\boldsymbol{\omega}}_i + \sum_{k=1}^{r-2} \mathbf{Q}_i^{(k)} \hat{\boldsymbol{\omega}}_i^{(k)} + \\ & k \{ [\sum_{j \in \mathcal{N}} a_{ij}(\mathbf{q}_i - \mathbf{q}_j) + a_{i0}(\mathbf{q}_i - \mathbf{q}_d)] \\ & + [\sum_{j \in \mathcal{N}} a_{ij}(\hat{\boldsymbol{\omega}}_i - \hat{\boldsymbol{\omega}}_j) + a_{i0}(\hat{\boldsymbol{\omega}}_i - \boldsymbol{\omega}_d)] \}] \end{aligned} \quad (24)$$

where $\mathbf{Q}_i^{(k)}$ denotes the k^{th} time-derivative of the matrix \mathbf{Q}_i used in (5).

Theorem 2: Consider system (5) with $\mathbf{d}_i = 0$ and a sliding function of the form (21). If there exists a constant $k > 0$, then the protocols (24) guarantee that $\lim_{t \rightarrow T} (\mathbf{q}_i - \mathbf{q}_j) = 0$ and $\lim_{t \rightarrow T} (\boldsymbol{\omega}_i - \boldsymbol{\omega}_j) = \lim_{t \rightarrow T} (\boldsymbol{\omega}_i - \boldsymbol{\omega}_d) = 0$, where T is the synchronization time.

Proof: Let $e_0 = z_0 - f(t)$ be the differentiation error, then system (23) can be written as

$$\begin{cases} \dot{e}_0 = e_1 - \mu_0 |e_0|^{-\frac{1}{r}} e_0 \\ \dot{e}_1 = e_2 - \mu_1 |e_0|^{-\frac{1}{r-1}} e_0 \\ \vdots \\ \dot{e}_{r-2} = e_{r-1} - \mu_{r-2} |e_0|^{-\frac{1}{2}} e_0 \\ \dot{e}_{r-1} = -\mu_{r-1} |e_0|^{-1} e_0 - f^{(r)} \end{cases} \quad (25)$$

The error dynamics (25) can be set in the following pseudo linear system form

$$\dot{\mathbf{e}} = \mathbf{A}\mathbf{e} + \mathbf{b}f^{(r)} \quad (26)$$

with

$$\mathbf{e} = [e_0 \ e_1 \ \dots \ e_{r-1}]^T, \quad \mathbf{b} = [0 \ 0 \ \dots \ 1]^T$$

$$\mathbf{A} = \begin{bmatrix} -\mu_0 |e_0|^{-\frac{1}{r}} & 1 & 0 & \dots & 0 \\ -\mu_1 |e_0|^{-\frac{1}{r-1}} & 0 & 1 & \ddots & 0 \\ \vdots & \vdots & \vdots & \ddots & \vdots \\ -\mu_{r-2} |e_0|^{-\frac{1}{2}} & 0 & 0 & \dots & 1 \\ -\mu_{r-1} |e_0|^{-1} & 0 & 0 & \dots & 0 \end{bmatrix}$$

One can easily find that the determinant of matrix \mathbf{A} is given as

$$\det(\mathbf{A}) = (-1)^r \mu_{r-1} |e_0|^{-1} = \prod_{i=1}^r \bar{\lambda}_i \quad (27)$$

and its characteristic polynomial as

$$p_A(\lambda) = \det(\mathbf{A} - \lambda \mathbf{I}) = \sum_{k=1}^r \lambda^{r-k} (-1)^k \text{tr}(\wedge^k \mathbf{A}) \quad (28)$$

where λ denotes an eigenvalue of \mathbf{A} and $(\wedge^k \mathbf{A})$ denotes the trace of the k^{th} exterior power of \mathbf{A} . Equation (28) gives

$$p_A(\lambda) = \lambda^r + \mu_0 |e_0|^{-\frac{1}{r}} \lambda^{r-1} + \mu_1 |e_0|^{-\frac{1}{r-1}} \lambda^{r-2} + \dots + \mu_{r-1} |e_0|^{-1} \quad (29)$$

The polynomial (29) is stable if its coefficients satisfy the following Schur condition

$$1 > \mu_0 |e_0|^{-\frac{1}{r}} > \mu_1 |e_0|^{-\frac{1}{r-1}} > \dots > \mu_{r-1} |e_0|^{-1} > 0 \quad (30)$$

To fulfill condition (30), the differentiator coefficients μ_i are computed using the following tuning recursive scheme

$$\begin{cases} \mu_0 := \alpha L^{1/r} \\ \mu_i := \mu_{i-1} L^{1/(r-i)} \quad (i = 1, \dots, r - 1) \end{cases} \quad (31)$$

where $\alpha \in \mathbb{R}^+$ is a tuning parameter. According to the scheme (31), for any $r > 1$ and Lipschitz constant $L \in \mathbb{R}^+$, $\exists \alpha$ such that $\mu_0 < 1$. Consequently, condition (30) is guaranteed, and matrix A is stable.

End of proof.

IV. SIMULATION

In this section, numerical simulations are performed to confirm the above theoretical results and prove the performance and effectiveness of the proposed control scheme. The distributed torque laws (7) and (24) and the observer (23) were applied to a four-satellite formation that runs under an undirected switching communication topology shows in Fig. 1. Table I gives the moments of inertia and the initial conditions of the four satellites.

TABLE I. PARAMETERS OF THE SATELLITES

Sat.	Initial attitude/angular velocity (rad/s)	Moment of inertia (kg.m ²)
1	$q_1 = [0.5916, 0.6, -0.5, -0.2]$ $\omega_1 = [0.02, -0.01, -0.02]$	$J_1 = \text{diag}[10.15, 10.20, 9.85]$
2	$q_2 = [0.7874, 0.5, -0.3, -0.2]$ $\omega_2 = [0.03, -0.01, -0.01]$	$J_2 = \text{diag}[12.1, 10.90, 10.50]$
3	$q_3 = [0.6245, 0.3, -0.6, -0.4]$ $\omega_3 = [0.02, 0.00, -0.03]$	$J_3 = \text{diag}[9.55, 12.30, 10.20]$
4	$q_4 = [0.6403, 0.5, -0.3, -0.5]$ $\omega_4 = [-0.01, 0.02, -0.03]$	$J_4 = \text{diag}[10.50, 11.20, 10.20]$

First, the satellites are required to align their attitudes to the desired $\bar{q}_d = (0, 0, 0, 1)^T$ and $\omega_d = (0, 0, 0)^T$. The distributed torque law (7) is applied with $k = 3.7$, and the simulation is run under the communication topology shown in Fig. 1 for a 60 s with a dwell time $\tau = 15$ s. Fig. 2 and 3 depict the quaternions and angular velocities tracking errors, and Fig. 4 shows the required control torques.

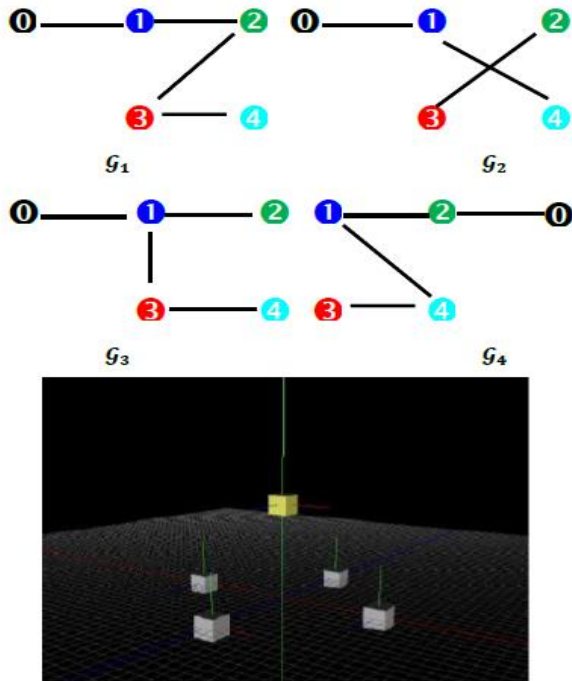


Fig. 1. Switching interaction topology among a four-satellite formation.

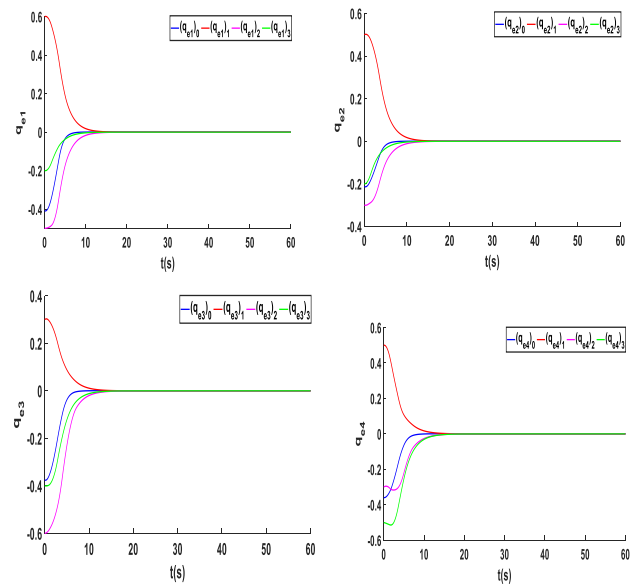


Fig. 2. Quaternions tracking errors.

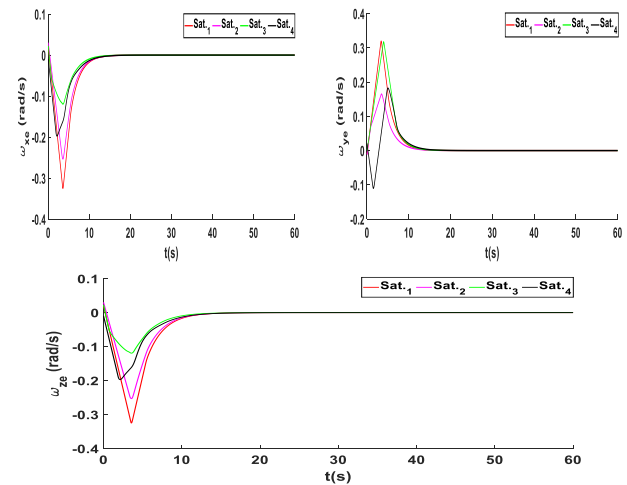


Fig. 3. Angular velocity tracking errors.

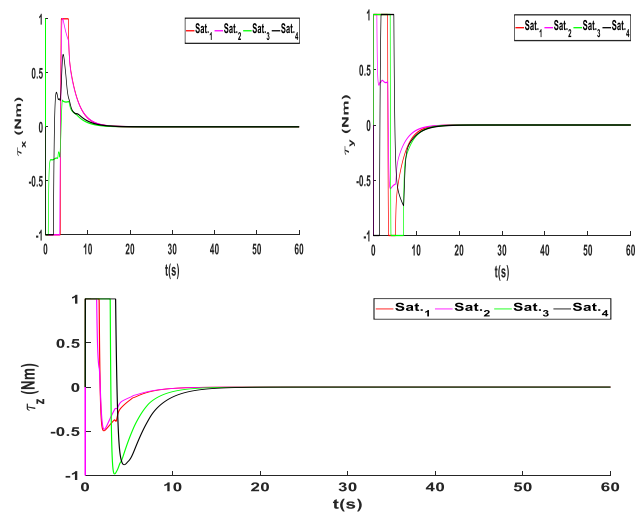


Fig. 4. Control efforts (torques).

The results above indicate that the four satellites can align their attitude to the specified one while effectively maintaining the consensus (6) despite the ISCLS' failures. Next, the case of attitude synchronization without angular velocity measurement is considered. In this scenario, the efficiency of the redesigned torque law (24) with a third-order observer (23) is verified. An external disturbance of $\mathbf{d} = 10^{-4}[\sin(0.12t), \sin(0.5t), \sin(0.18t)]^T$ is introduced to the system (5). The simulation is run with $k = 1.2, \alpha = 0.15$, under the leaderless communication topology shown in Fig. 5. Fig. 6 shows the relative attitude $\mathbf{q}_{ij} = \mathbf{q}_j^* \mathbf{q}_i$ where \mathbf{q}_j^* denotes the cross-product matrix associated with the quaternion vector \mathbf{q}_j . The relative angular velocity errors $\boldsymbol{\omega}_{ei} = \boldsymbol{\omega}_i - \boldsymbol{\omega}_j$ are depicted in Fig. 7.

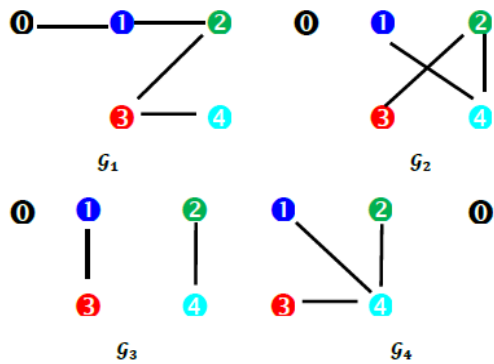


Fig. 5. Switching interaction topology among a four-satellite formation with loss of the leader.

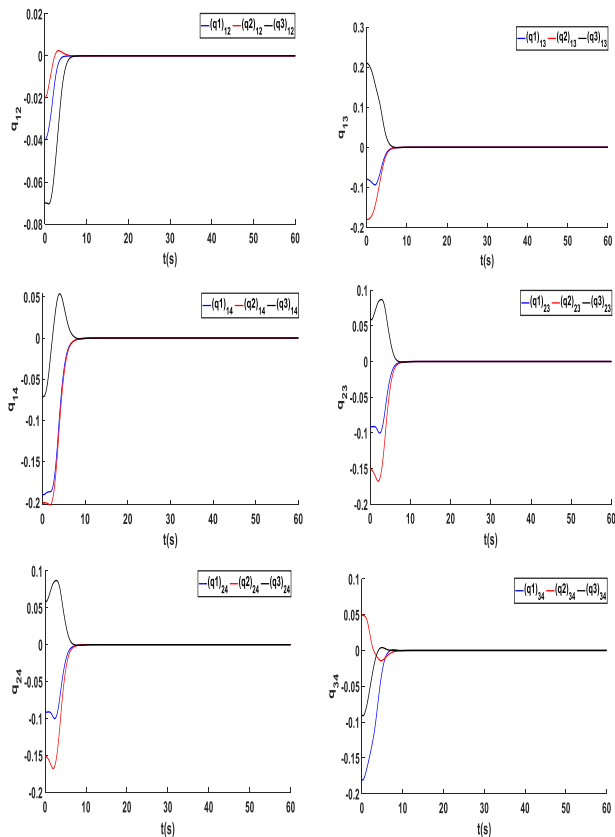


Fig. 6. Relative satellite-to-satellite attitude errors.

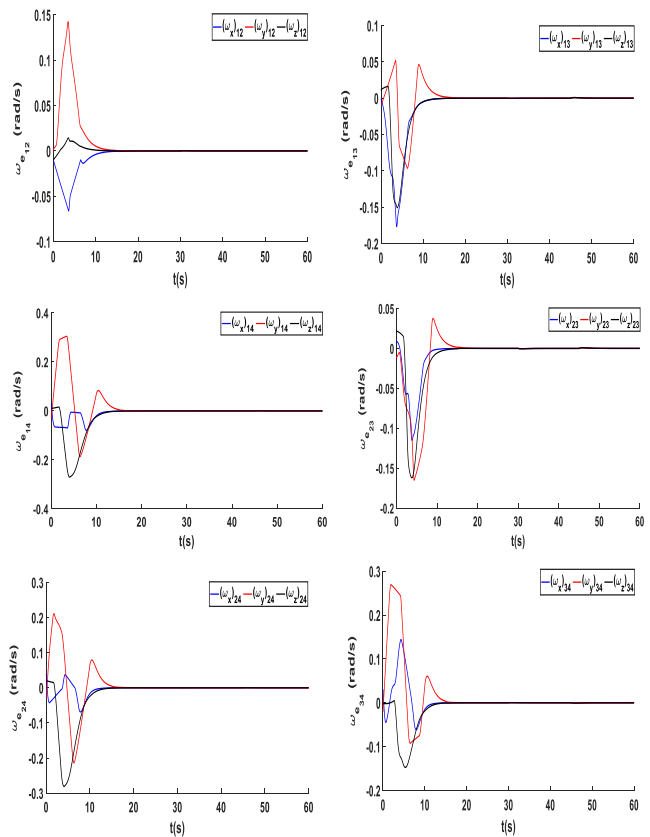


Fig. 7. Relative satellite-to-satellite angular speed errors.

For a fair comparison, attitude synchronization paths for satellites using second and third-order sliding mode observers are shown in Fig. 8.

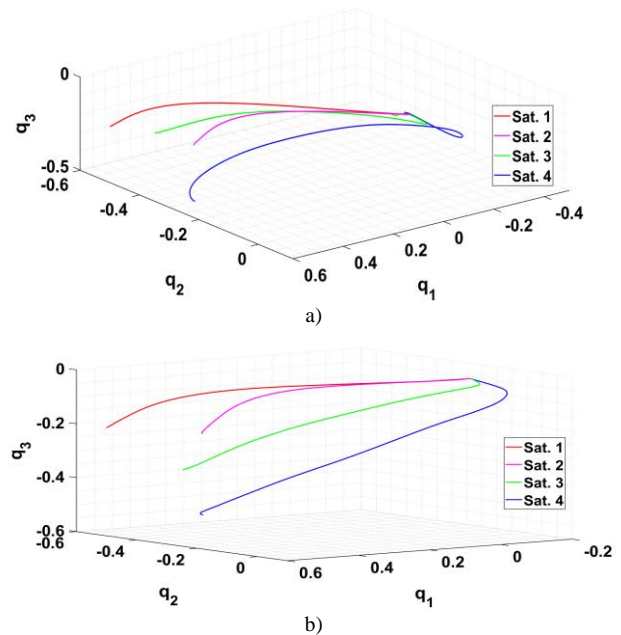


Fig. 8. Attitude synchronization paths with a) second-order observer, b) third-order observer.

Using both static and dynamic communication topologies with and without velocity measurements, the results of the present research demonstrated the feasibility and effectiveness of the proposed finite-time attitude synchronization for satellite formation systems. The results showed that instead of using the actual measured angular velocities, the designed observer with a finite-time high-order sliding-mode generated high-precision estimates. The observer was implemented to lessen the load on the inter-satellite communication lines and guarantee the formation's resilience in the face of link failures. In addition, the performance of the augmented control law (24) is shown to be satisfactory by comparing Fig. 2 and 3 and Fig. 6 and 7. This is the case despite the fact that estimations of relative angular velocities are utilized, as well as the fact that external disturbances are implemented. In addition, it can be shown from Fig. 8 that raising the order of the observer can result in an increase in the precision of the attitude synchronization.

V. CONCLUSION

This paper has investigated the finite-time attitude synchronization for satellite formation systems under switching communication topologies with and without velocity measurements. First, Lyapunov-based distributed torque laws were designed to provide a coordinated synchronization of the states of following satellites with the desired attitudes and angular speeds. The distributed protocols were developed using graph theory, local finite-time convergence for homogeneous systems, and non-smooth LaSalle's invariance principle. Then, a finite-time high-order sliding-mode observer was designed to provide relative angular velocity estimates instead of the measured ones. The distributed observer is introduced to reduce the inter-satellite communication links burden and ensure formation robustness against their breaks. Future works will focus on solving some critical inter-satellite transmission problems such as signal overriding, signal interferences, and communication delays.

ACKNOWLEDGMENT

This project was funded by the Deanship of Scientific Research (DSR) at King Abdulaziz University, Jeddah, under grant no. (G:305-135-1441). The authors, therefore, acknowledge with thanks DSR for technical and financial support.

REFERENCES

- [1] S. Bandyopadhyay, R. Foust, G.P. Subramanian, S-J Chung, F.Y Hadaegh, Review of formation flying and constellation missions using nanosatellites, *Journal of Spacecraft and Rockets* 53 (3) (2016) 567–578. <https://doi.org/10.2514/1.A33291>
- [2] J. Sullivan, S. Grimberg, S. D'Amico, Comprehensive survey and assessment of spacecraft relative motion dynamics models, *Journal of Guidance, Control, and Dynamics*. 40 (8) (2017) 1-23. <https://doi.org/10.2514/1.G002309V>
- [3] VLS. Freitas, F.L. de Sousa, E.E.N. Macau, Reactive model for autonomous vehicles formation following a mobile reference, *Applied Mathematical Modelling*. 61 (2018) 167-180. <https://doi.org/10.1016/j.apm.2018.04.011>
- [4] L.M. Marrero, et al., Architectures and synchronization techniques for distributed satellite systems: a survey, *IEEE Access*. (2022). <https://doi.org/10.48550/arXiv.2203.08698>
- [5] O. Mechali, L. Xu, X. Xie, J. Iqbal, Theory and practice for autonomous formation flight of quadrotors via distributed robust sliding mode control

- protocol with fixed-time stability guarantee, *Control Engineering Practice*. 123 (2022) 105150 <https://doi.org/10.1016/j.conengprac.2022.105150>
- [6] D. Wang, B. Wu, and E.K., Poh, Satellite formation flying: Relative dynamics, formation design, fuel optimal maneuvers and formation maintenance, Springer (2017), DOI 10.1007/978-981-10-2383-5
- [7] S. Mathavaraj and R.Padhi, Satellite formation flying: High precision guidance using optimal and adaptive control techniques, Springer (2021) <https://doi.org/10.1007/978-981-15-9631-5>
- [8] J. Zhou, et al., Decentralized finite time attitude synchronization control of satellite formation flying, *Journal of Guidance, Control, and Dynamics* 36 (1) (2013) 185–195. <https://doi.org/10.2514/1.56740>
- [9] L. Zhao, Y. Jia, Decentralized adaptive attitude synchronization control for spacecraft formation using nonsingular fast terminal sliding mode, *Nonlinear Dynamics* 78 (2014) 2779–2794. DOI:10.1007/s11071-014-1625-5
- [10] Z. Wang, et al., Decentralized attitude synchronization of spacecraft formations under complex communication topology, *Advances in Mechanical Engineering* 8 (8) (2016) 1–12. <https://doi.org/10.1177/1687814016660464>
- [11] J. Zhang, Q. Hu, W. Xie, Integral sliding mode-based attitude coordinated tracking for spacecraft formation with communication delays, *International Journal of Systems Science* 48 (15) (2017) 3254-3266. <https://doi.org/10.1080/00207721.2017.1371359>
- [12] J. Zhang, D. Ye, J.D. Biggs, Z. Sun, Finite-time relative orbit-attitude tracking control for multi-spacecraft with collision avoidance and changing network topologies, *Advances in Space Research* 63 (2019) 1161-1175. <https://doi.org/10.1016/j.asr.2018.10.037>
- [13] H. Liu, Y. et al., Robust formation flying control for a team of satellites subject to nonlinearities and uncertainties, *Aerospace Science and Technology*. 95 (2019) 105455. <https://doi.org/10.1016/j.ast.2019.105455>
- [14] X. Liu., Y. Zou, Z. You, Coordinated attitude synchronization and tracking control of multiple spacecraft over a communication network with a switching topology, *IEEE Transactions on Aerospace and Electronic Systems* 56 (2) (2020) 1148-1162. DOI: 10.1109/TAES.2019.2925512
- [15] M. Lu L. Liu, Leader-following attitude consensus of multiple rigid spacecraft systems under switching networks, *IEEE transactions on automatic control* 65 (2) (2020) 839-845. DOI: 10.1109/TAC.2019.2920074
- [16] X. Zhang, et al., Finite-time distributed attitude synchronization for multiple spacecraft with angular velocity and input constraints, *IEEE Transactions on Control Systems Technology* (2021). DOI: 10.1109/TCST.2021.3115479
- [17] S. Zhang, et al., General attitude cooperative control of satellite formation by set stabilization, *Acta Astronautica* 191 (2022) 125-133. <https://doi.org/10.1016/j.actaastro.2021.10.043>
- [18] C. Wei, et al., An overview of prescribed performance control and its application to spacecraft attitude system, *Journal of Systems and Control Engineering* (2020) 1-3. <https://doi.org/10.1177/0959651820952552>
- [19] Q. Hu, J. Zhang, Y. Zhang, Velocity-free attitude coordinated tracking control for spacecraft formation flying, *ISA Transactions* 73 (2018) 54-65, <https://doi.org/10.1016/j.isatra.2017.12.019>
- [20] M. Xu, Y. et al., Chattering free distributed consensus control for attitude tracking of spacecraft formation system with unmeasurable angular velocity, *International Journal of Control, Automation, and Systems*, 18 (9), (2020), 2277-2288. <http://dx.doi.org/10.1007/s12555-019-0543-1>
- [21] H. Yi, Y. Jia, Adaptive finite time distributed 6-DOF synchronization control for spacecraft formation without velocity measurement, *Nonlinear Dynamics* 95 (2019), 2275–2291. <https://doi.org/10.1007/s11071-018-4691-2>
- [22] M. Liu, A. Zhang, B. Xiao, Velocity-free state feedback fault-tolerant control for satellite with actuator and sensor faults, *Symmetry* 14 (157). <https://doi.org/10.3390/sym14010157>
- [23] H. Yang, X. You, C. Hua, Attitude tracking control for spacecraft formation with time-varying delays and switching topology, *Acta*

- Astronautica 126 (2016) 98-108. <https://doi.org/10.1016/j.actaastro.2016.04.012>
- [24] R. Horn, C. Johnson, *Topics in Matrix Analysis*, Cambridge University Press (1991), Cambridge.
- [25] A. Levant, Higher order sliding modes differentiation and output-feedback control, *International Journal of Control*. 76 (9/10) (2003) 924–941. <https://doi.org/10.1080/0020717031000099029>